ORIGINAL ARTICLE

Effects of hyperbaric environment on endurance and metabolism are exposure time-dependent in well-trained mice

Junichi Suzuki [ID]

Laboratory of Exercise Physiology, Health and Sports Sciences, Course of Sports Education, Department of Education, Hokkaido University of Education, Iwamizawa, Japan

Correspondence
Junichi Suzuki, Laboratory of Exercise Physiology, Health and Sports Sciences, Course of Sports Education, Department of Education, Hokkaido University of Education, Midorigaoka, Iwamizawa, Hokkaido, Japan.
Email: suzuki.junichi@i.hokkyodai.ac.jp

Abstract

Hyperbaric exposure (1.3 atmospheres absolute with 20.9% O_2) for 1 h a day was shown to improve exercise capacity. The present study was designed to reveal whether the daily exposure time affects exercise performance and metabolism in skeletal and cardiac muscles. Male mice in the training group were housed in a cage with a wheel activity device for 7 weeks from 5 weeks old. Trained mice were then subjected to hybrid training (HT, endurance exercise for 30 min followed by sprint interval exercise for 30 min). Hyperbaric exposure was applied following daily HT for 15 min (15HT), 30 min (30HT), or 60 min (60HT) for 4 weeks. In the endurance capacity test, maximal work values were significantly increased by 30HT and 60HT. In the left ventricle (LV), activity levels of 3-hydroxyacyl-CoA-dehydrogenase, citrate synthase, and carnitine palmitoyl transferase (CPT) 2 were significantly increased by 60HT. CPT2 activity levels were markedly increased by hyperbaric exposure in red gastrocnemius (Gr) and plantaris muscle (PL). Pyruvate dehydrogenase complex activity values in PL were enhanced more by 30HT and 60HT than by HT. Protein levels of N-terminal isoform of PGC1α (NT-PGC1α) protein were significantly enhanced in three hyperbaric exposed groups in Gr, but not in LV. These results indicate that hyperbaric exposure for 30 min or longer has beneficial effects on endurance, and 60-min exposure has the potential to further increase performance by facilitating fatty acid metabolism in skeletal and cardiac muscles in highly trained mice. NT-PGC1α may have important roles for these adaptations in skeletal muscle.

KEYWORDS
bayesian data analysis, hybrid exercise, hyperbaric exposure, left ventricle, NT-PGC1α, skeletal muscle

1 | INTRODUCTION

Athletes with a broad range of performance levels use a commercial hyperbaric apparatus, which functions at <1.5 atmospheres absolute (ATA) with room air (20.9% O_2). Acute hyperbaric exposure (1.3 ATA) for 1 h markedly up-regulated mRNA expression levels of proliferator-activated receptor gamma coactivator 1-alpha (PGC1α) and peroxisome proliferator-activated receptor alpha (PPARα) in hind-leg muscles 3 h after exposure (Suzuki, 2017). Moreover, endurance exercise training followed by hyperbaric exposure for daily 1 h markedly improved both fatty acid and glucose metabolism in hind-leg muscles in highly trained mice (Suzuki, 2019a). To apply daily hyperbaric exposure to

human athletes, the duration of exposure should be shorter, and should not disturb the daily training regimen. Acute hyperbaric exposure (1.3 ATA with room air) for 30 min after maximal exercise markedly reduced the lactate concentration and heart rate in humans (Park et al. 2018). However, an additive effect of hyperbaric exposure on exercise performance has not yet been reported in terms of the daily exposure time.

High-intensity interval exercise (6 × 30-sec all-out cycling) followed by endurance exercise (60% VO_2max for 60 min) markedly enhanced mRNA levels of PGC1α compared with those observed after respective, single, uncombined regimens in trained human muscle (Skovgaard et al. 2016). Hybrid exercise training (HT) consisting of interval and endurance exercise may be beneficial to improve the endurance capacity of highly trained individuals. HT (endurance exercise for 30 min followed by sprint interval exercise (5-s run-10-s rest) for 30 min) for 4 weeks enhanced the endurance capacity, but endurance training did not, in mice that were trained from an early age (Suzuki, 2019b).

In a previous study, in highly trained mice, hyperbaric exposure identically enhanced exercise-induced PGC1α protein levels in the nucleus, but the levels of facilitation were statistically insignificant (Suzuki, 2019a). Muscle-specific deletion of PGC1α and β did not affect training-induced exercise performance (Ballmann et al. 2016). N-terminal isoform of PGC1α (NT-PGC1α) was shown to have the regulatory role in mitochondrial biogenesis and adaptation of skeletal muscle induced by endurance exercise (Wen et al. 2014). Thus, detecting NT-PGC1α protein levels may clarify one of mechanisms underlying hyperbaric exposure-induced adaptation.

Although hyperbaric exposure for 1 h markedly facilitated exercise-induced muscle hypertrophy in mice (Suzuki, 2019a), mechanisms underlying these changes have yet to be clearly determined. In previous studies, levels of heat shock protein (HSP) 70 were upregulated by endurance training with hyperbaric exposure in hind-leg muscles (Suzuki, 2017, 2019a). HSP70 was shown to have an important role in the recovery of skeletal muscle after intensive exercise (McArdle et al. 2004). AKT, also known as protein kinase B (PKB), is a serine/threonine protein kinase with multiple regulatory functions, including the control of cell growth, survival, apoptosis, proliferation, angiogenesis, and the metabolism of carbohydrates, lipids and proteins (Risso et al. 2015). AKT1 was shown to have a crucial role in regulating satellite cell proliferation during skeletal muscle hypertrophy (Moriya et al. 2018).

Most ATP production in the heart depends on fatty acid oxidation (Gibb & Hill, 2018). Fat metabolism in the heart was shown to decrease after chronic endurance training (Gibb & Hill, 2018) and interval training (Hafstad et al. 2011). However, no study has observed enzyme activity levels concerning fatty acid metabolism after chronic exercise training with hyperbaric exposure.

In the present study, experiments were designed to elucidate the effects of HT with different durations of hyperbaric exposure on exercise capacity as well as protein levels involved in muscle growth and mitochondrial biogenesis, and metabolic enzyme activity levels in skeletal and cardiac muscles of well-trained mice.

2 | MATERIALS AND METHODS

2.1 | Ethical approval

All procedures were approved by the Animal Care and Use Committee of Hokkaido University of Education (No. 3, approved on 2019/4/16) and performed in accordance with the "Guiding Principles for the Care and Use of Animals in the Field of Physiological Sciences" of the Physiological Society of Japan and the 'European Convention for the Protection of Vertebrate Animals used for Experimental and other Scientific Purposes' (Council of Europe No. 123, Strasbourg, 1985).

2.2 | Animals, hyperbaric exposure, and exercise training

Fifty male ICR (MCH) mice (four weeks old) were purchased from Clea Japan Inc. and housed under the conditions of a controlled temperature (24 ± 1°C) and relative humidity of approximately 50%. Lighting (7:00–19:00) was controlled automatically. All mice were given commercial laboratory chow (solid CE-2, Clea Japan) and tap water *ad libitum*. After mice had been fed for one week and allowed to adapt to the new environment, they were randomly assigned to a sedentary control group (Sed, n = 10) or training group (n = 40). Mice in the training group were individually housed in a cage with a wheel activity device (13 cm in diameter) for 7 weeks, as described previously (Suzuki, 2019a). Wheel activity (distance and running time) was monitored and recorded using digital bike computers (CC-VL820, Cateye Co., Ltd.). Mice in the Sed group were housed individually throughout the experiment. To familiarize mice with the treadmill device, all mice including the Sed group were subjected to treadmill walking once a week using a controlled treadmill (Modular motor assay, Columbus Instruments Inc.) for 5 min per day at 10–15 m min^{-1} with a 5-deg incline.

Running distance during voluntary wheel training is shown in Figure 1. Following voluntary wheel training, mice were given a 48-h non-exercise period prior to the maximal endurance capacity test. The test was performed with a graded ramp running protocol using the controlled treadmill, as described previously (Suzuki, 2019b). Total work (joules) was calculated as a product of body weight (kg), speed (m
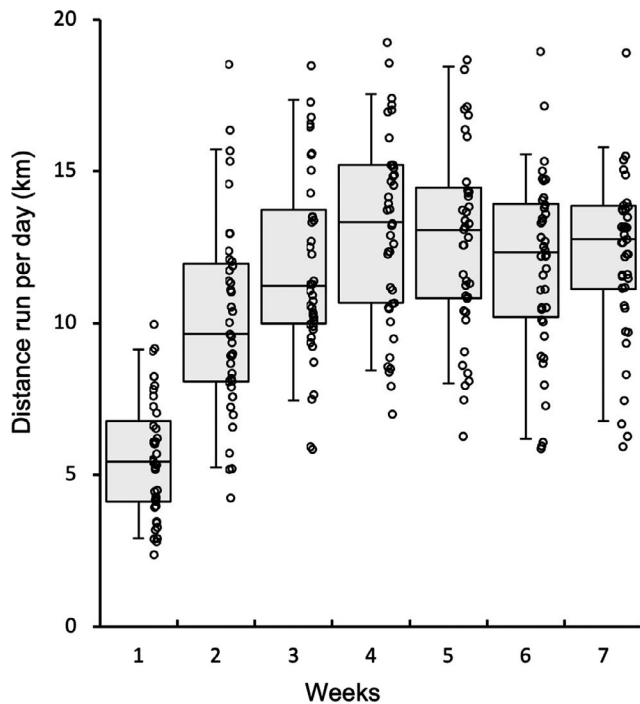
FIGURE 1 Running distance per day during voluntary wheel training. Values are expressed as box and whisker plots with 5th, 25th, 50th, 75th and 95th percentile. Dots are individual data points.
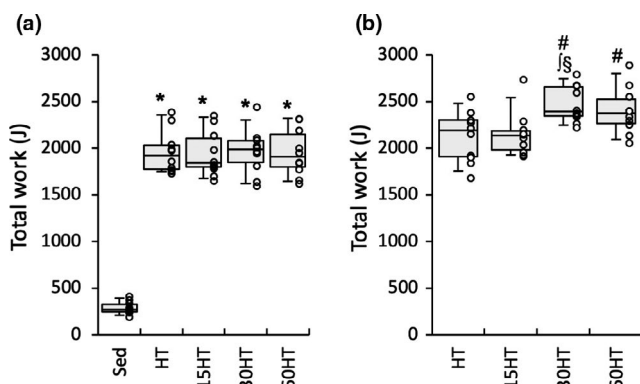
FIGURE 2 Endurance exercise performance test. Total work capacity of the endurance capacity test after 7 weeks of voluntary wheel running (a) and after 4 weeks of treadmill exercise training (b) #, significantly different from pre-treadmill training values of each group shown in the panel (a). *, ∫, and §, significantly different from Sed, HT, and 15HT groups, respectively. Values are expressed as box and whisker plots with 5th, 25th, 50th, 75th and 95th percentile. Dots are individual data points.

sec^{-1}), time (sec), slope (%), and 9.8 (m sec^{-2}). Exhaustion was defined when the mouse stayed for more than 5 s on the metal grid (no electrical shock) at the rear of the treadmill, despite external gentle touch being applied to their tail with a conventional elastic bamboo stick (0.8 mm in diameter).

Following the performance test, mice were given a 48-h non-exercise period prior to treadmill training. Mice in the

training group were divided into a hybrid-training group (HT, n = 10), hybrid-training group with hyperbaric exposure for 15 min daily (15HT, n = 10), 30 min daily (30HT, n = 10), or 60 min daily (60HT, n = 10), in order to match the mean and SD values of total work (Figure 2a). During the period of HT, mice were housed individually in a cage without a wheel device. Mice in the training groups were subjected to HT in a normobaric environment 6 days per week for 4 weeks (within 2 h from approximately 5 AM) using a rodent treadmill (KN-73, Natsume Co.). Instead of using an electrical shock, the tail or feet of mice were touched with a conventional test tube brush made of soft porcine bristles in order to motivate them to run when they stayed on a metal grid for more than 2 s. HT consists of endurance exercise for 30 min followed by an interval exercise regimen (5-sec run-10-sec rest) for 30 min interposed by a 5-min rest. For endurance exercise, mice ran at 20 m min^{-1} with a 15-deg incline on the first and second days of training. The running speed was increased to 25 and 27.5 m min^{-1} on the first and fourth days of the second week, respectively, and to 30 m min^{-1} on the second day of the third week. For the interval exercise regimen, mice ran at 30 m min^{-1} with a 15-deg incline on the first day of training. The running speed was increased to 35, 37.5, 40, and 42.5 m min^{-1} on the 4th, 7th, 10th, and 13th days of training, respectively. The maximal endurance capacity test was performed 48 h after the last run, as described above.

The hyperbaric exposure group was subjected to 1.3 ATA with room air (20.9% O$_2$) for 15, 30, or 60 min, once per day (started at approximately 30 min after daily exercise), 6 days per week, for 4 weeks. The hyperbaric exposure was performed as described previously (Suzuki, 2019a). The pressure of the chamber was gradually increased or decreased at 0.136 ATA min^{-1} within 2.2 min.

Forty-eight hours after the last run, mice were anesthetized with α-chloralose (0.06 g kg^{-1} i. p. Wako Pure Chemical Industries Ltd.) and urethane (0.7 g kg^{-1} i. p. Wako). A toe pinch response was used to validate adequate anesthesia. The plantaris (PL) and gastrocnemius muscles were excised and the deep red region (Gr) of the gastrocnemius was isolated from the superficial white region (Gw). The diaphragm (DIA) was excised. All samples were frozen in liquid nitrogen for biochemical analyses. The remaining muscles, i.e., those on the right side, were excised and placed in embedding medium, O.C.T. compound (Miles Inc.), and then rapidly frozen in isopentane cooled to its melting point (−160°C) with liquid nitrogen. Mice were killed by excision of the heart. The whole heart and left ventricle (LV) were weighed and frozen in liquid nitrogen. All tissue samples were stored at −80°C until for analyses.

2.3 | Histological analyses

Histochemical examinations of capillary profiles and muscle fiber phenotypes were conducted as previously reported by

the author with slight modifications (Suzuki, 2019b). Briefly, ten-micrometer-thick serial cross-sections were obtained using a cryotome (CM-1500; Leica Japan Inc.) at −20°C from the mid-belly portion of calf muscles. These sections were air-dried, fixed with 100% ethanol at 4°C for 15 min, and then washed in 0.1 M phosphate-buffered saline (PBS) with 0.1% Triton X-100. Sections were then blocked with 10% goat normal serum at room temperature for 30 min, washed in PBS for 5 min, and incubated at 4°C overnight with a mixture of fluorescein-labeled Griffonia simplicifolia lectin (GSL I) (FL 1101 (1:100), Vector Laboratories Inc.), an anti-type I myosin heavy chain (MHC) antibody (BA-F8, mouse IgG2b, 1:80), and anti-type IIA MHC antibody (SC-71, mouse IgG1, 1:80) diluted with PBS. Sections were then reacted with a secondary antibody mixture containing Alexa Fluor 350-labeled anti-mouse IgG2b (1:100) and Alexa Fluor 647-labeled anti-mouse IgG1 (1:100) diluted with PBS at room temperature for 1 h. Sections were coverslipped with Fluoromount/Plus (K048, Diagnostic BioSystems Co.). Primary and secondary antibodies were purchased from the Developmental Studies Hybridoma Bank (University of Iowa) and Thermo Fisher Scientific Inc, respectively. Fluorescent images of the incubated sections were observed using a microscope (Axio Observer, Carl Zeiss Japan). Muscle fiber phenotypes were classified as type I (blue), type I+IIA (faint blue and faint red), type IIA (red), type IIAX (faint red), and type IIB+IIX (unstained). Representative immunofluorecent images are shown in Figure 3. Non-overlapping microscopic fields were selected at random from each muscle sample. The observer was blinded to the source (groups) of each slide during the measurements. Fluorescent images were obtained from PL, the lateral (GrL) and medial (GrM) portions of Gr, and Gw. Fiber cross-sectional area (FCSA) values were obtained using public domain Image J software (NIH, Bethesda). The negative control without primary antibodies was confirmed to show no fluorescent signal.

2.4 | Biochemical analyses of enzyme activities

Frozen tissue powder was obtained using a frozen sample crusher (SK mill, Tokken Inc.,) and homogenized with ice-cold medium (10 mM HEPES buffer, pH 7.4; 0.1% Triton X-100; 11.5% (w/v) sucrose; and 5% (v/v) protease inhibitor cocktail (P2714, Sigma-Aldrich)) in a ultrasonic bath (43 kHz, 50 W) at 4°C for 5 min. After centrifugation at $1500 \times g$ at 4°C for 10 min, the supernatant was used in enzyme activity analyses. The activities of 3-hydroxyacyl-CoA-dehydrogenase (HAD) and lactate dehydrogenase (LDH) were assayed according to the method of Bass et al. (1969). Assay for cytochrome oxidase (COX) activities were prepared according to the method of Sherratt et al. (1988). The activities of citrate synthase (CS) and phosphofructokinase (PFK) were assayed according to the method of Srere (1969) and Passonneau and Lowry (1993), respectively. Pyruvate dehydrogenase complex (PDHc) activity was measured by the phenazine methosulfate-3-(4, 5-dimethylthiazol-2-yl)-2,5-diphenyltetazolium bromide (PMS-MTT) assay (Ke et al. 2014). For the carnitine palmitoyl transferase (CPT) 2 assay, the tissue homogenate was added to the reaction medium (200 mM HEPES, 10 mM EGTA, 0.2 M sucrose, 400 mM KCl, 2 mM DTNB (Sigma O4126), 0.13% (w/v) bovine serum albumin (Wako 017–15146), 20 μM palmityl CoA (Sigma P 9716), 10 μM malonyl CoA (Sigma M4263)) and incubated for 1 h in a dark chamber at 25 ºC. After confirming there was no non-specific reaction, the reaction was initiated
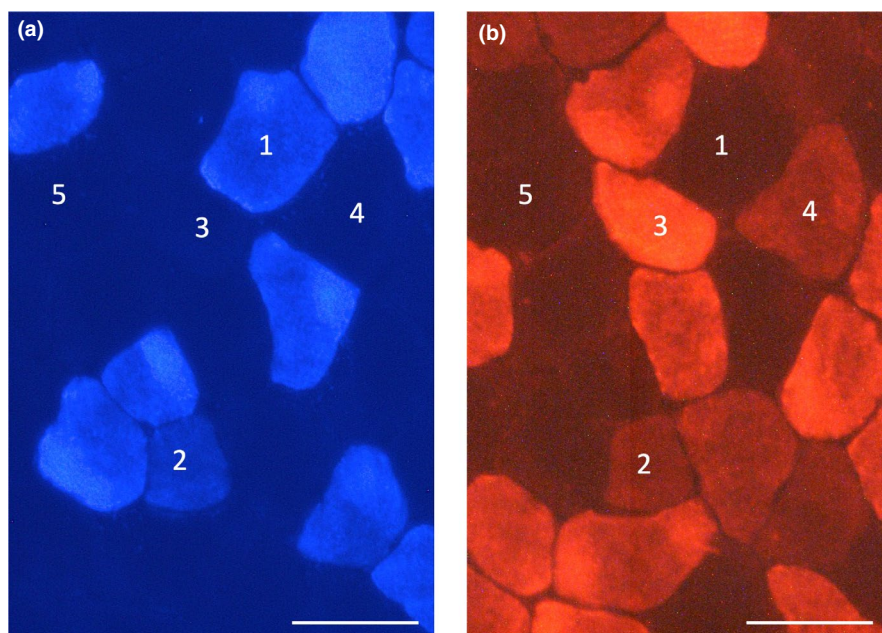
FIGURE 3 Representative immunofluorecent images of type I (a) and type IIA (b) muscle fibers. 1, type I fiber; 2, type I+IIA fiber; 3, type IIA fiber; 4, type IIAX fiber; 5, type IIB+IIX fiber. Horizontal bars represent 50 μm.

by adding 15 mM L-carnitine (Sigma C0283). All measurements were conducted at 25°C with a spectrophotometer (U-2001, Hitachi Co.) and enzyme activities were obtained as µmol h^{-1} mg protein^{-1}. Total protein concentrations were measured using PRO-MEASURE protein measurement solution (iNtRON Biotechnology Inc.).

2.5 | Western blot analyses

The tissue homogenates described above were used for Western blot analyses. A sample (50 µg) was fractionated by SDS/PAGE on 12% (w/v) polyacrylamide gels (TGX StainFree FastCast gel, Bio-Rad Inc.), exposed to UV for 1 min and total protein patterns were visualized using ChemiDoc MP Imager (Bio-Rad). The stain-free gel contains a trihalo compound which reacts with proteins during separation, rendering them detectable using UV exposure (Gilda &Gomes, 2013; Vigelsø et al. 2014). Then, gels were electrophoretically transferred to a polyvinylidene fluoride (PVDF) membrane. The bands in each lane on the membrane were detected with ChemiDoc MP and the images were used for normalization process as described below. The blots were blocked with 3% (w/v) bovine serum albumin (protease and IgG free, 010–25783 Fujifilm Wako Pure Chemical, Osaka Japan), 1% (w/v) polyvinylpyrrolidone (PVP40, Sigma-Aldrich), and 0.3% (v/v) Tween-20 in PBS for 1 h, and then exposed to a specific primary antibody (1:500, Santa Cruz Biotechnology Inc.) against AKT1 (sc-5298), HSP70 (1:500, sc-66048), TFAM (sc-166965), MFN2 (sc-100560), FABP (sc-514208), or DRP1 (1:500, sc-271583) diluted in PBS with 0.05% Tween-20 (PBST) for 1 h. After the blots had been incubated with a HRP-labeled mouse IgGκ light chain binding protein (1:5000, sc-516102, Santa Cruz), they were reacted with Clarity Western ECL substrate (Bio-Rad), Clarity Max Western ECL substrate (Bio-Rad), or their mixture and the required proteins were detected with ChemiDoc MP. The densities of the specific bands were quantified using Image Lab software (Bio-Rad) and normalized to the densities of all protein bands in each lane on the membrane (Figure 4a). (Gilda & Gomes, 2013; Vigelsø et al. 2014). Then, the normalized densities of the bands were normalized again to the same sample that was run on every gel and transferred to every membrane (STD in Figure 4).

For detecting nuclear levels of PGC1α and NT- PGC1α proteins in Gr and LV, nuclear proteins were extracted using around 20 mg of tissue. After cytosolic proteins were extracted as described in the previous section, the pellet was suspended in ice-cold buffer (0.2 M HEPES buffer, pH 7.4; 1.5 mM MgCl$_2$; 420 mM NaCl; 25% glycerol (v/v); and 5% (v/v) protease inhibitor cocktail (Sigma-Aldrich)) and rotate at 4°C for 20 min. After centrifugation at $18{,}000 \times g$ at 4°C for 20 min, the supernatant was collected and 40 µg of protein
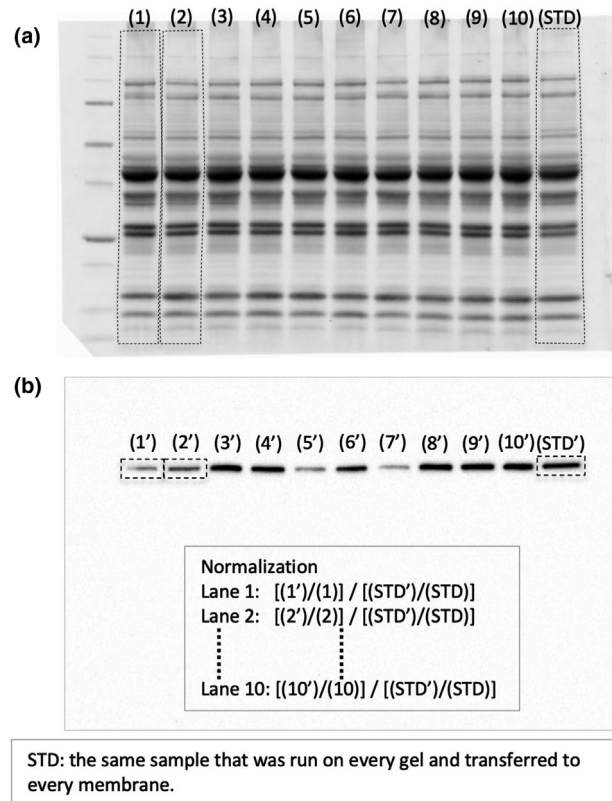
FIGURE 4 Normalization method for Western blot analyses. (a) Example image of PVDF membrane after electrical blotting for detecting total protein that were transferred. (b) Example image after immunodetecting of specific bands.

was used for western blot analyses. The blots were blocked with 5% (w/v) non-fat dry milk (sc-2325, Santa Cruz) in PBST for 1 h, and then exposed to anti-PGC1α primary antibody (1:1000, sc-518025, Santa Cruz) diluted in PBST for 1 h. Incubation for secondary antibody and detection of specific bands were done as described above.

2.6 | Statistical analyses

According to the statement of American Statistical Association (Wasserstein & Lazar, 2016), the present study used the Bayesian estimation for statistical analysis, instead of p value as in null hypothesis significance testing, such as ANOVA and post hoc test.

Differences between the two groups were examined using Bayesian estimation with a gamma prior distribution proposed by Kruschke (2015). The posterior distribution was obtained using the Markov chain Monte Carlo (MCMC) methods. Public domain R, RStudio, and JAGS programs were used for computing Bayesian inference. The MCMC chains were considered to show a stationary distribution when the Gelman-Rubin values (shrink factor) were less than 1.10 for all parameters. The significance of differences

was evaluated by the 95% highest density interval (HDI) and a region of practical equivalence (ROPE) (Kruschke, 2018). When the HDI value on the effect size fell outside of the ROPE set at −0.1 to 0.1, the difference was regarded as significant (Kruschke, 2018; Kruschke & Liddell, 2018).

Bayesian robust linear regression (Kruschke, 2015) was used to establish any correlation between the parameters observed in the present study. The regression was considered significant when HDI on the slope fell outside of the ROPE. Data are expressed as box and whisker plots with 5th, 25th, 50th,

TABLE 1 Body and organ masses

	Sed (n = 10)	HT (n = 10)	15HT (n = 10)	30HT (n = 10)	60HT (n = 10)
Body mass (g)					
Pre-HT	38.3 ± 1.7	36.1 ± 3.4	36.3 ± 0.95	35.0 ± 1.7	36.2 ± 1.1
Post-HT	41.0 ± 1.7	37.5 ± 2.0[a]	38.1 ± 0.9[a]	38.4 ± 1.7[a]	38.4 ± 1.2[a]
Post-Pre difference	2.71 ± 1.16	1.45 ± 1.77	1.81 ± 1.12	3.35 ± 1.15	2.19 ± 1.17
Organ mass (mg)					
Gastrocnemius	178.6 ± 12.1	174.3 ± 8.9	171.4 ± 7.1	171.2 ± 8.1	175.2 ± 10.2
Plantaris	21.8 ± 1.1	23.1 ± 1.9	22.7 ± 2.2	23.7 ± 1.7	23.3 ± 3.1
Whole heart	158.1 ± 10.9	178.1 ± 12.3[a]	182.6 ± 9.6[a]	187.5 ± 10.6[a]	183.3 ± 8.1[a]
Left ventricle	114.3 ± 8.9	128.4 ± 9.9[a]	133.3 ± 7.6[a]	136.2 ± 8.7[a]	137.1 ± 14.3[a]
Organ mass-to-body mass ratio (mg g^{-1})					
Gastrocnemius	4.36 ± 0.29	4.65 ± 0.26	4.50 ± 0.21	4.46 ± 0.21	4.56 ± 0.17
Plantaris	0.53 ± 0.04	0.62 ± 0.06	0.60 ± 0.06	0.62 ± 0.04	0.61 ± 0.08
Whole heart	3.87 ± 0.18	4.75 ± 0.22[a]	4.79 ± 0.18[a]	4.88 ± 0.21[a]	4.76 ± 0.12[a]
Left ventricle	2.79 ± 0.15	3.42 ± 0.16[a]	3.49 ± 0.14[a]	3.55 ± 0.18[a]	3.56 ± 0.37[a]

Values are presented as means ± SD.

[a]significantly different from the Sed group using Bayesian estimation. Pre-HT and Post-HT, at the beginning and end, respectively, of the 4 weeks of HT.
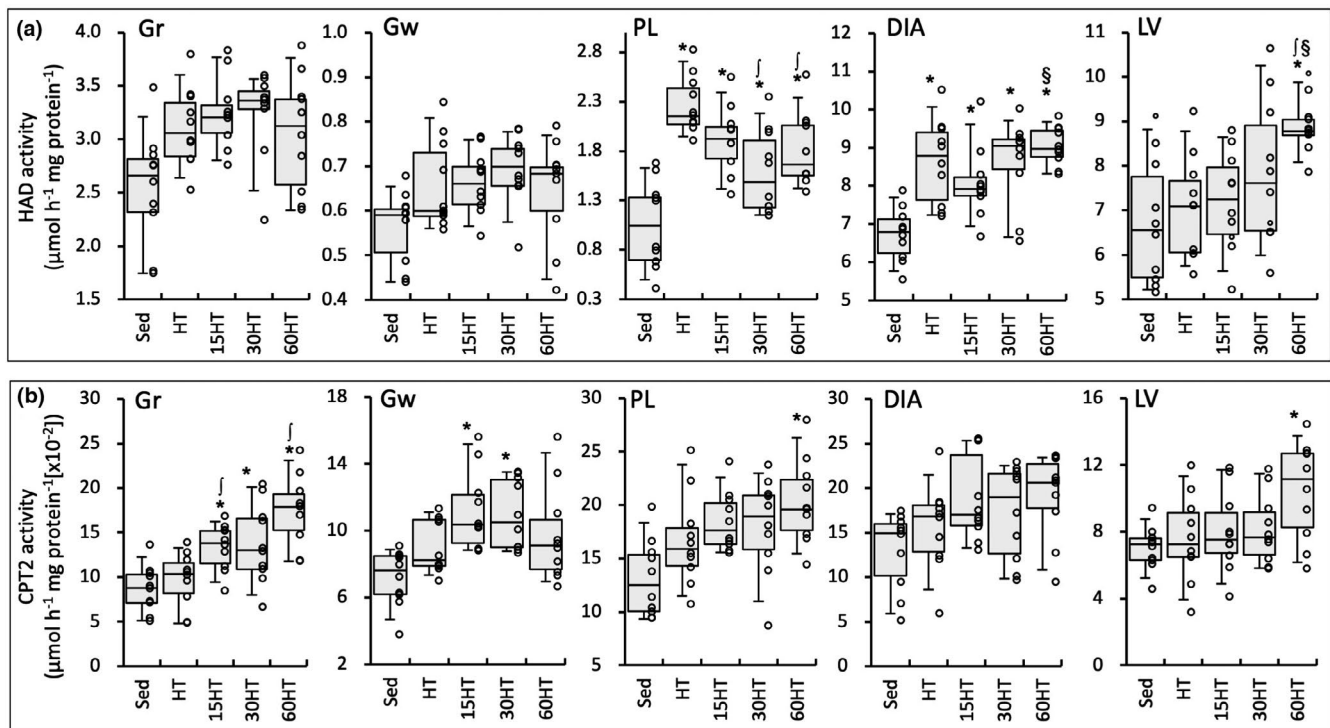
FIGURE 5 Enzyme activity values for HAD (a) and CPT2 (b). Values are expressed as box and whisker plots with 5th, 25th, 50th, 75th and 95th percentile. Dots are individual data points. *, ∫, and §, significantly different from Sed, HT, and 15HT groups, respectively.

TABLE 2 Correlations

Explanatory variable	Response variable	Gr	Gw	PL	DIA	LV
LDH	Maximal work[b]	a	ns	ns	ns	ns
PDHc	Maximal work[b]	ns	ns	a	ns	ns
CPT2	Maximal work[b]	ns	ns	ns	a	ns
CS	Maximal work[b]	ns	ns	ns	a	ns
HAD	Maximal work[b]	ns	ns	ns	ns	ns
COX	Maximal work[b]	ns	ns	ns	ns	ns
PFK	Maximal work[b]	ns	ns	ns	ns	ns
DRP1	Maximal work[b]	ns	ns	ns	ns	ns
MFN2	Maximal work[b]	ns	ns	ns	ns	ns
TFAM	Maximal work[b]	ns	ns	ns	ns	ns
AKT1	Maximal work[b]	ns	ns	ns	ns	ns
HSP70	Maximal work[b]	ns	ns	ns	ns	ns
FABP	Maximal work[b]	ns	ns	ns	ns	ns
PGC1α	Maximal work[b]	ns				ns
NT-PGC1α	Maximal work[b]	ns				ns
C:F ratio	Maximal work[b]	ns	ns	ns		
Capillary density	Maximal work[b]	ns	ns	ns		
AKT1	Total FCSA	ns	ns	a	ns	ns
AKT1	C:F ratio	ns	ns	a	ns	ns
HSP70	Total FCSA	ns	a	ns	ns	ns
DRP1	COX	a	a	ns	a	a
DRP1	CS	a	a	a	a	a
DRP1	HAD	a	a	a	a	a
DRP1	CPT2	ns	a	ns	ns	ns
TFAM	COX	a	a	ns	ns	ns
TFAM	CS	a	a	ns	ns	a
TFAM	HAD	a	a	a	ns	a
MFN2	COX	ns	ns	a	ns	ns
MFN2	CS	a	ns	ns	ns	ns
MFN2	HAD	ns	ns	a	ns	ns
NT-PGC1α	CS	a				ns
NT-PGC1α	COX	a				ns
NT-PGC1α	TFAM	a				ns

Correlations were established using Bayesian robust linear regression.

[a]significant correlation; ns, non-significant correlation.

[b]Correlations were calculated without Sed group.

75th, and 95th percentile in the figures and means $\pm$ standard deviation (SD) in Table 1.

3 | RESULTS

3.1 | Body and organ masses

Body weight values after HT were significantly lower in the four exercise-trained groups than in Sed group (Table 1).

However, body weight values before HT and the amount of increase during HT were not significantly different among groups. The absolute and relative weight values of the whole heart and LV were significantly higher in the four exercise-trained groups than in the Sed group. The relative weight values of GAS and PL were higher in the four exercise-trained groups than in the Sed group, but the differences were not significant. Thus, hyperbaric exposure did not affect the body weight or HT-induced cardiac and skeletal muscle growth.

3.2 | Maximal exercise capacity

After voluntary wheel running for 7 weeks, total work values were significantly greater in the training group by 6.9-fold (Figure 2a) than in Sed group. In 30HT and 60HT groups, total work values were significantly increased after 4 weeks of treadmill training. Moreover, total work values were significantly greater in the 30HT group than in HT and 15HT groups (Figure 2b). Thus, daily hyperbaric exposure longer than 30 min had additive effects on HT-induced improvements in endurance capacity.

3.3 | Metabolic enzyme activities

CPT2 activity values in Gr were significantly higher in the three exposure groups than in the Sed group and, moreover, the values were significantly higher in 15HT and 60HT groups than in the HT group (Figure 5b). In PL and LV, CPT2 activity levels showed significantly higher values in the 60HT group than in the Sed group. CPT2 activity values in Gw were significantly higher in 15HT and 30HT groups than in the Sed group. In DIA, CPT2 values were positively correlated with maximal work values (Table 2).

HAD activity values in LV were significantly higher in 60HT than in Sed, HT, and 15HT groups (Figure 5a). In PL,

HAD levels were significantly lower in 30HT and 60HT groups than in the HT group, while activity values showed significantly greater values in the four training groups than in the Sed group.

While COX activity values in Gr and PL were markedly increased after exercise training, the values were significantly higher in the 15HT than in the HT group in Gr (Figure 6a). In Gw, COX levels were significantly greater in three hyperbaric-treated groups than in the Sed group. CS activity values in LV were significantly higher in the 60HT than in Sed and 15HT groups (Figure 6b). In DIA, a positive correlation was observed between CS levels and maximal work values (Table 2).

PDHc activity values in PL were significantly higher in 30HT and 60HT groups than in Sed, HT, and 15HT groups (Figure 7a). Moreover, in PL, a positive correlation was found between PDHc levels and maximal work values (Table 2). In Gw, PDHc activity levels showed significantly greater values in 15HT, 30HT, and 60HT groups than in Sed and HT groups, and the levels were significantly greater in the 60HT group than in the 15HT group. In DIA, PDHc activity values were significantly higher in 15HT and 30HT groups than in the HT group. PDHc activity levels in LV showed significantly lower values in the 15HT group than in Sed and HT groups.

In 30HT and 60HT groups, LDH activity values were significantly higher and lower, respectively, in Gr and LV,
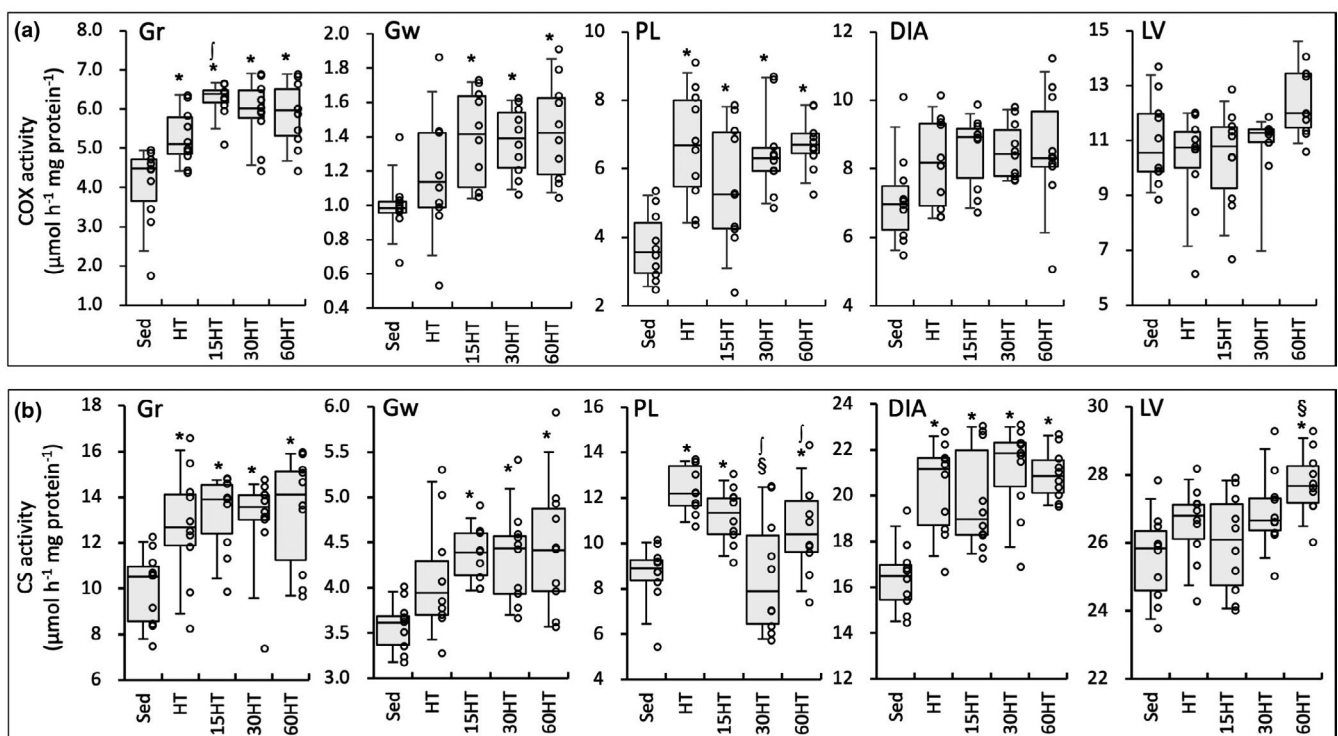
FIGURE 6 Enzyme activity values for COX (a) and CS (b). Values are expressed as box and whisker plots with 5th, 25th, 50th, 75th and 95th percentile. Dots are individual data points. *, ∫, and §, significantly different from Sed, HT, and 15HT groups, respectively.

than in Sed, HT, and 15HT groups (Figure 7b). LDH activity values were positively correlated with maximal work values in Gr (Table 2).

Thus, 60HT enhanced the activities of enzymes involved in mitochondrial fatty acid as well as glucose metabolism in hindleg and cardiac muscles, whereas 30HT predominantly enhanced glucose metabolism in the hindleg muscles.

3.4 | Protein levels

TFAM abundance in Gr was significantly stronger in the four training groups than in the Sed group (Figure 8c). TFAM levels in PL were significantly higher in HT and 60HT groups

than in the Sed group. Expression levels of TFAM were significantly correlated with COX, CS, and HAD activity levels in Gr and Gw (Table 2). MFN2 protein levels in PL were markedly stronger in the four training groups than in the Sed group (Figure 8b).

AKT1 protein levels in PL were significantly stronger in the four training groups than in the Sed group (Figure 9b). AKT1 expression levels in PL were positively correlated with total FCSA values (Table 2).

HSP70 levels in Gr were significantly stronger in the four training groups than in the Sed group (Figure 9c). In Gw, HSP70 protein levels were significantly stronger in HT, 15HT, and 30HT groups than in the Sed group. HSP70 levels in Gw tended to be greater (1.6-fold) in the 60HT group than in the Sed group. HSP70 levels in DIA were significantly
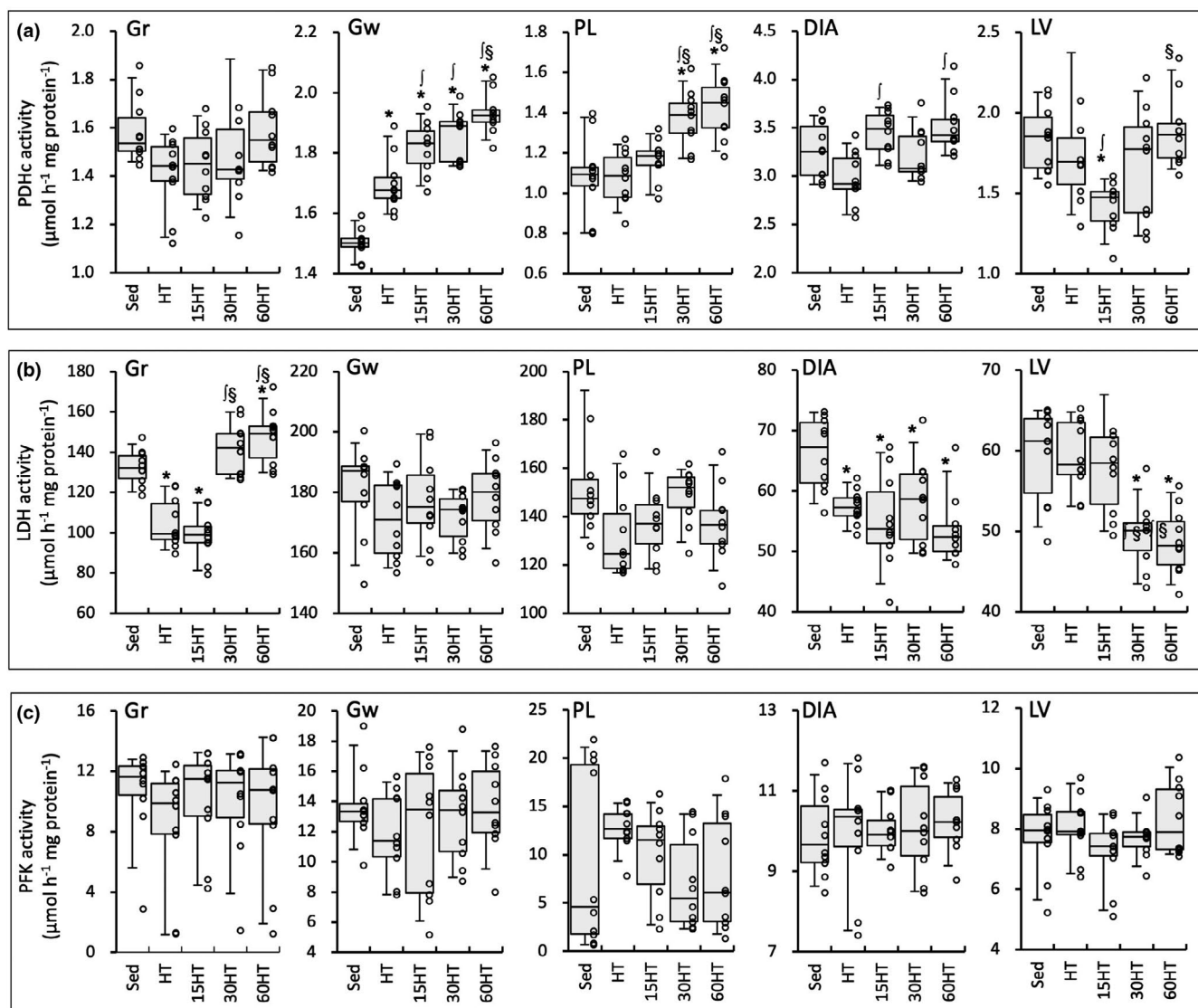
FIGURE 7 Enzyme activity values for PDHc (a), LDH (b), and PFK (c). Values are expressed as box and whisker plots with 5th, 25th, 50th, 75th and 95th percentile. Dots are individual data points. *, ∫, and §, significantly different from Sed, HT, and 15HT groups, respectively.
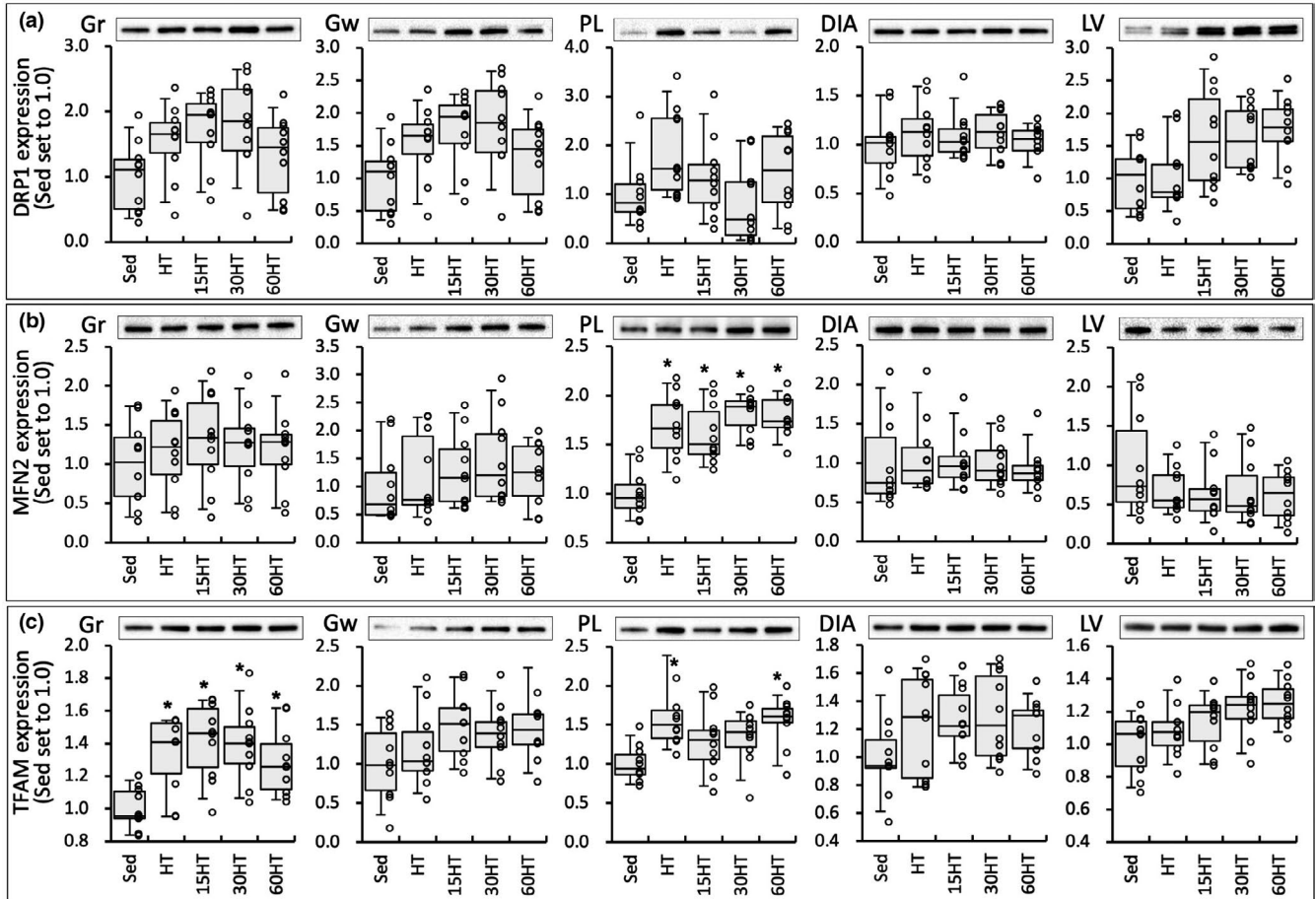
FIGURE 8 Protein levels of DRP1 (a), MFN2 (b), and TFAM (c). Values are expressed as box and whisker plots with 5th, 25th, 50th, 75th and 95th percentile. Dots are individual data points. *, significantly different from the Sed group.

stronger in 15HT and 30HT groups than in the Sed group. HSP70 levels were positively correlated with total FCSA values in Gw (Table 2).

Nuclear NT-PGC1α protein levels in Gr showed significantly stronger values in the three hyperbaric exposure groups than in the Sed group (Figure 10a). Moreover, the levels were markedly greater in 15HT (by 22%), 30HT (by 30%), and 60HT (by 25%) groups than in HT group. Significant correlations were observed between NT-PGC1α expression levels and CS, COX, and TFAM values in Gr (Table 2).

3.5 | Fiber-type composition

HT with and without hyperbaric exposure significantly increased the proportion of type IIA and IIAX fibers and decreased the proportion of type IIB+IIX fibers in PL (Figure 11). In GrL, the proportion of type IIAX fibers was larger and that of type IIB+IIX fibers was smaller in the four trained groups than in Sed group (Figure 11) . Thus, hyperbaric exposure did not affect the fiber proportion in hybrid-trained hindleg muscles.

3.6 | Fiber cross-sectional area

Total FCSA values in Gw were higher in the 60HT group than in Sed (by 16%) and 30HT (by 11%) groups, but the difference was not significant (Figure 12b). The distribution of total FCSA in the 60HT group was shifted to the larger fiber size in Gw (Figure 12a). Thus, hyperbaric exposure for 1 h partially promoted muscle fiber hypertrophy in highly glycolytic fibers.

3.7 | Capillarization

Capillary-to-fiber (C:F) ratio values in PL were significantly higher in the four trained groups than in the Sed group (Figure 13a). C:F ratio values in GrL and GrM were higher in the four training groups, but the differences were not significant. C:F values in Gw were markedly higher in the 60HT group than in the Sed group by 21%. Thus, daily hyperbaric exposure for 1 h markedly facilitated exercise-induced capillary growth in the muscle regions mainly composed of glycolytic fibers.
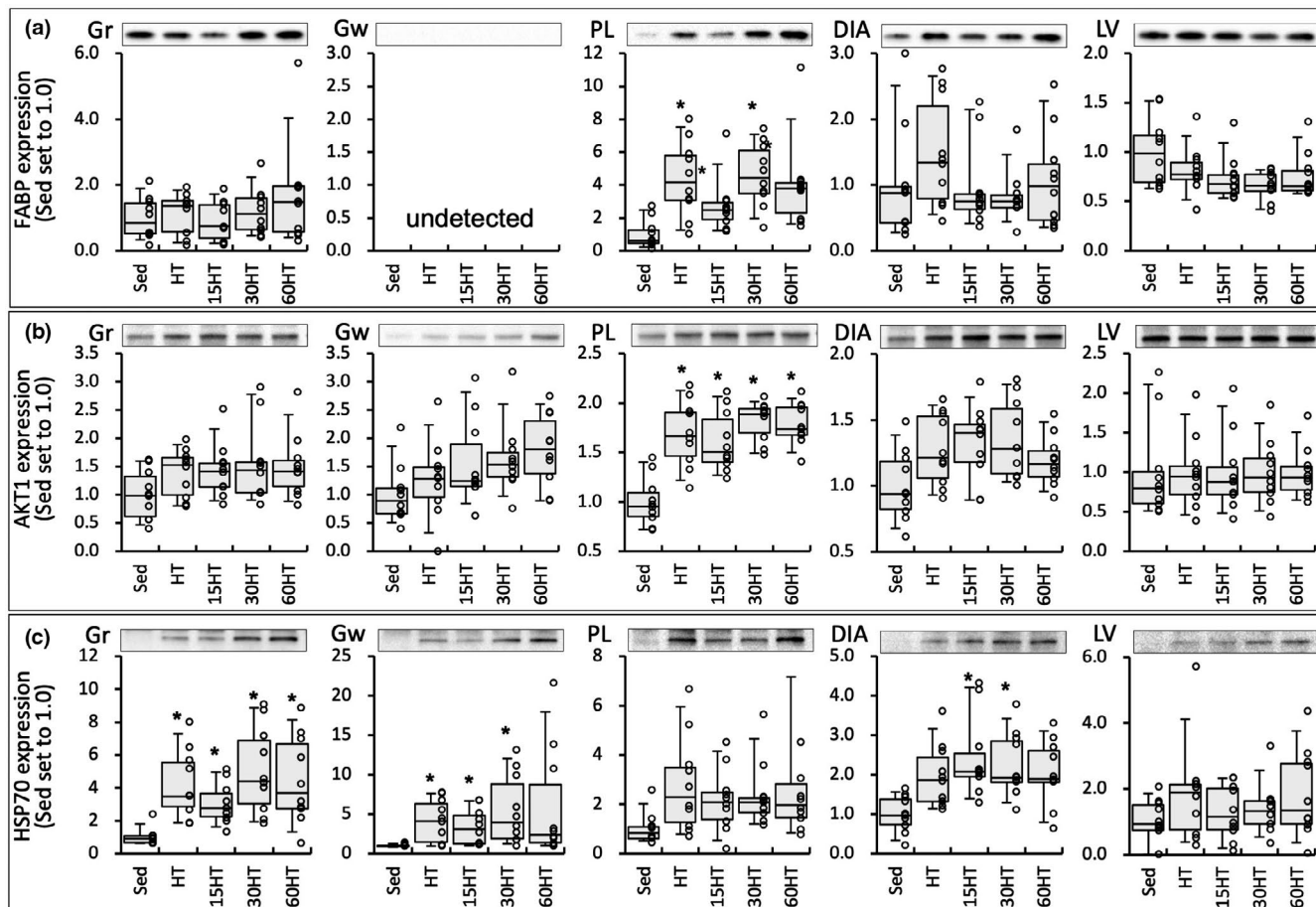
FIGURE 9 Protein levels of FABP (a), AKT1 (b), and HSP70 (c). Values are expressed as box and whisker plots with 5th, 25th, 50th, 75th and 95th percentile. Dots are individual data points. *, significantly different from the Sed group.

4 | DISCUSSION

In the present study, nuclear NT-PGC1α protein levels in Gr were markedly upregulated by hyperbaric exposure and an individual data in the groups indicated that the protein levels were increased with the duration of daily hyperbaric exposure (Figure 10a). Moreover, NT-PGC1α levels were significantly correlated with COX and CS activity levels and TFAM levels (Table 2). Thus, daily hyperbaric exposure with high-intensity training probably facilitated mitochondrial biogenesis and oxidative metabolism via NT-PGC1α upregulation in skeletal muscle.

In highly trained mice, in the present study, hyperbaric exposure with HT extensively enhanced CPT2 activity levels in hindleg muscles thereby promoting fatty acid metabolism (Figure 5b). Although regulatory mechanisms for CPT2 levels have not yet been clearly established, CPT1 levels were shown to be regulated by myocyte-specific enhancer factor (MEF2) (Yuan et al. 2014) and PPARα (Brandt et al. 2017). MEF2 was shown to activate PGC1α promotor (Czubryt et al. 2003), and PGC1α is one of cofactor of PPARα (Vega et al. 2000). Thus, upregulated

NT-PGC1α levels in the present study may upregulate the levels of CPTs. In a previous study, acute hyperbaric exposure at 1.3 ATA significantly enhanced mRNA levels of PGC1α and PPARα in hindleg muscles (Suzuki, 2017). However, daily hyperbaric exposure for 4 weeks with low intensity endurance training did not facilitate total CPT activity levels, while nuclear PGC1α levels were markedly enhanced (Suzuki, 2017). After 6 weeks of swimming training, high-intensity intermittent protocol significantly enhanced both CPT1 and CPT2 activity levels, while low intensity endurance protocol increased CPT1 levels but slightly reduced CPT2 levels (Carnevail et al. 2012). Thus, hyperbaric exposure with high-intensity hybrid exercise training used in the present study probably enhances both CPT1 and CPT2 levels via upregulating NT-PGC1α.

In highly trained mice, the present results showed that endurance exercise performance was promoted by HT with daily hyperbaric exposure for 30 and 60 min, but not for 15 min. In both 30HT and 60HT groups, additive effects of muscle metabolism were noted in PDHc activity values in PL and Gw, and in LDH activity values in Gr (Figure 7). Thus, daily hyperbaric exposure for 30–60 min had additive
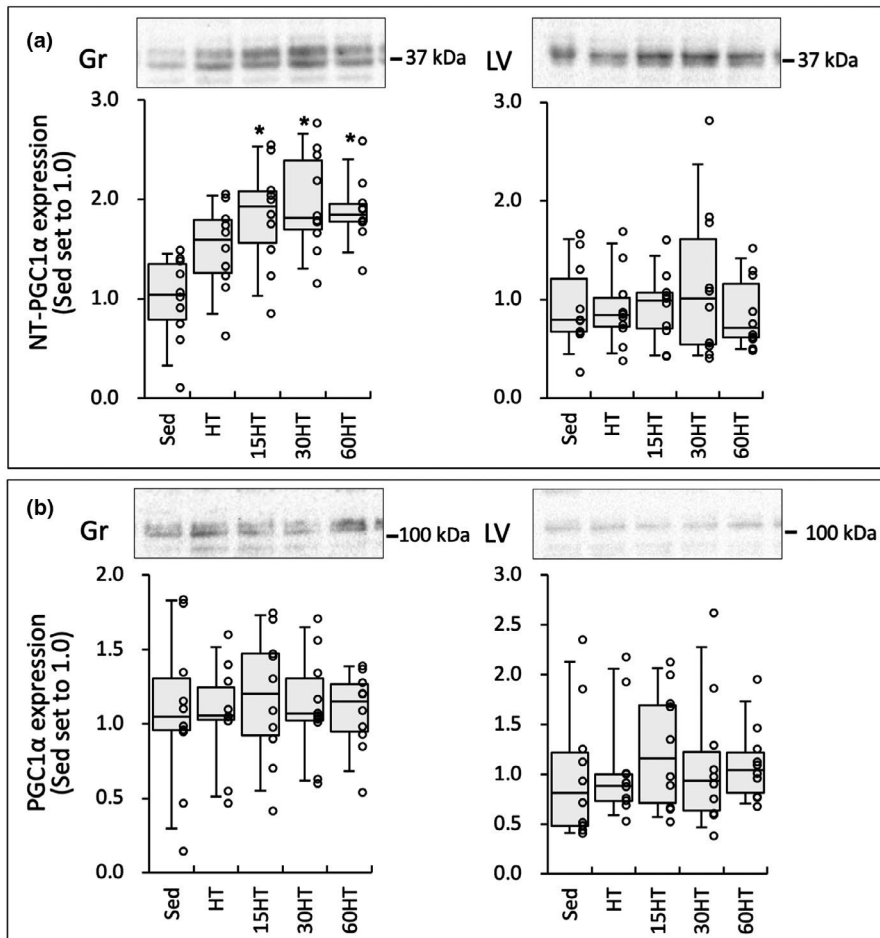
FIGURE 10 Protein levels of NT-PGC1α (a) and PGC1α (b) proteins in nuclear extracts. Values are expressed as box and whisker plots with 5th, 25th, 50th, 75th and 95th percentile. Dots are individual data points. *, significantly different from the Sed group.

effects on the training-induced increase in glucose metabolism in hindleg muscles. Endurance training with 60 min of hyperbaric exposure daily was shown to enhance PFK activity values, but did not change LDH activity values in hindleg muscle of highly trained mice (Suzuki, 2019A), suggesting that HT with hyperbaric exposure for at least 30 min daily may be beneficial to improve glucose metabolism in hindleg muscles.

In addition to these beneficial changes, HT with daily hyperbaric exposure for 60 min markedly enhanced cardiac fatty acid metabolism, identified by marked increases in HAD, CS, and CPT2 activity levels in LV (Figures 5 and 6). The present study is the first to report the effects of exercise training with hyperbaric exposure on cardiac metabolism. Around 95% of ATP used by cardiomyocytes is generated by oxidative phosphorylation in mitochondria (Gibb & Hill, 2018). Up to 70% of the oxidative metabolism principally relies on fatty acid oxidation (Gibb & Hill, 2018). However, fatty acid metabolism in the heart was not shown to be enhanced by chronic exercise training. After 5–6 weeks of endurance training, palmitoylcarnitine oxidation was shown to be significantly reduced in the heart, whereas it was unchanged in the gastrocnemius muscle of rats (Terblanche et al. 2001). Endurance training for

8 weeks did not increase palmitate oxidation while interval training (4-min run-2-min rest) decreased it in the mouse heart (Hafstad et al. 2011). Consistent with these findings, in the present study, HT itself did not affect enzyme levels concerning fatty acid metabolism in LV. Unfortunately, in the present study, protein levels of NT-PGC1 showed any change in LV (Figure 10a). Thus, the present results could not clearly explain the mechanisms underlying upregulated fatty acid metabolism in LV.

Glycolytic energy production by active skeletal muscles increases in proportion to exercise intensity, thereby increasing the plasma lactate concentration (Kemppainen et al. 2002). Myocardial lactate oxidation is prominent and proportional to the exogenous concentration during elevated workloads in rats (Allard et al. 1994). In isolated working rat hearts, lactate was found to contribute a relatively large proportion (up to 37%) of the total ATP supply under a low-fat condition (Schönekess, 1997). In contrast, under a high-fat condition, the contribution of lactate decreased to 13%, suggesting that fatty acid oxidation became a dominant source. This was supported by a study reporting that, in the perfused rat heart, rate values of triacyl glycerol degradation and total β-oxidation were markedly higher under high-fat and high-lactate conditions than low-fat and low-lactate conditions
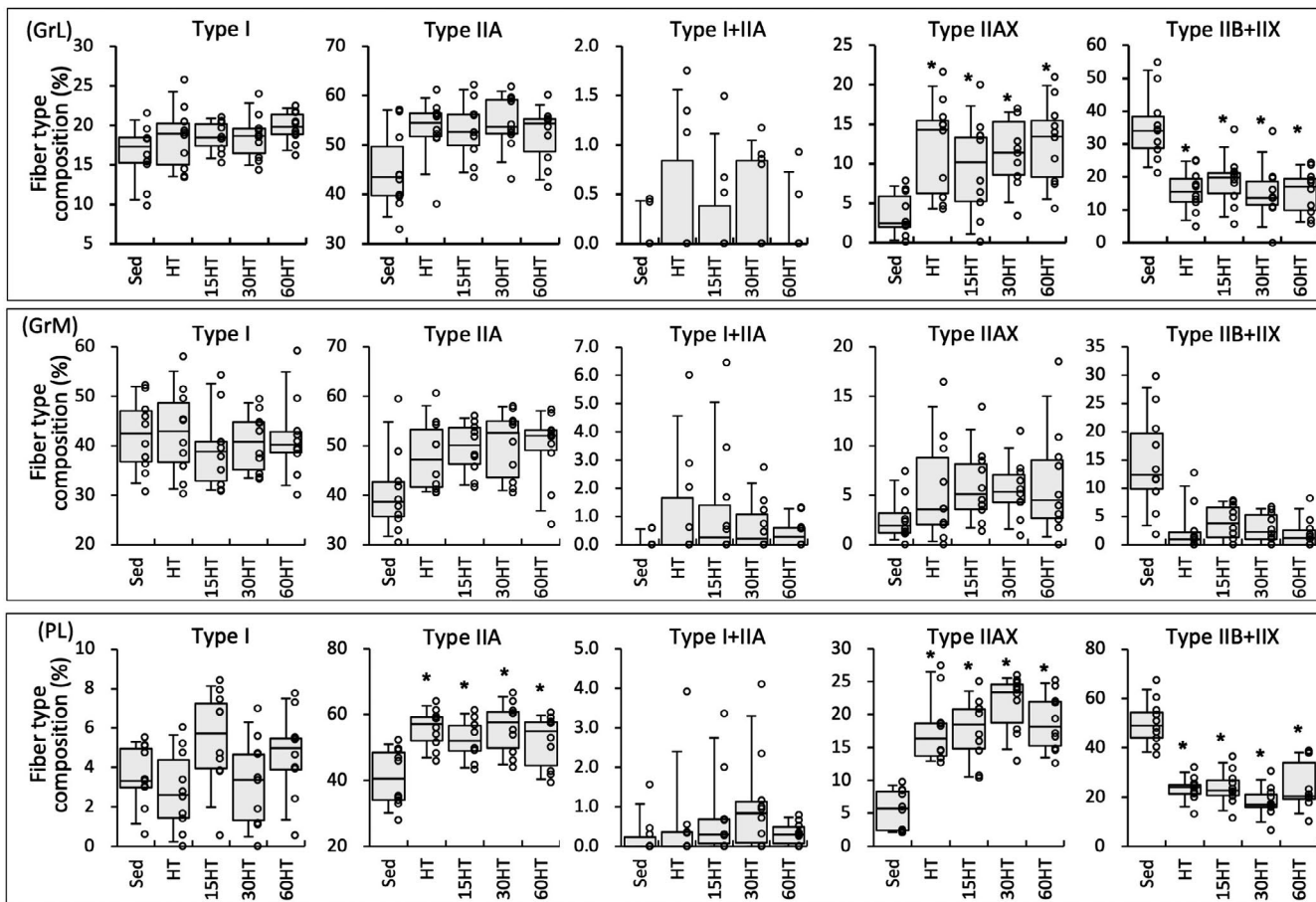
FIGURE 11 Fiber-type composition values in GrL (a), GrM (B), and PL (c) proteins. Values are expressed as box and whisker plots with 5th, 25th, 50th, 75th and 95th percentile. Dots are individual data points. *, significantly different from the Sed group.
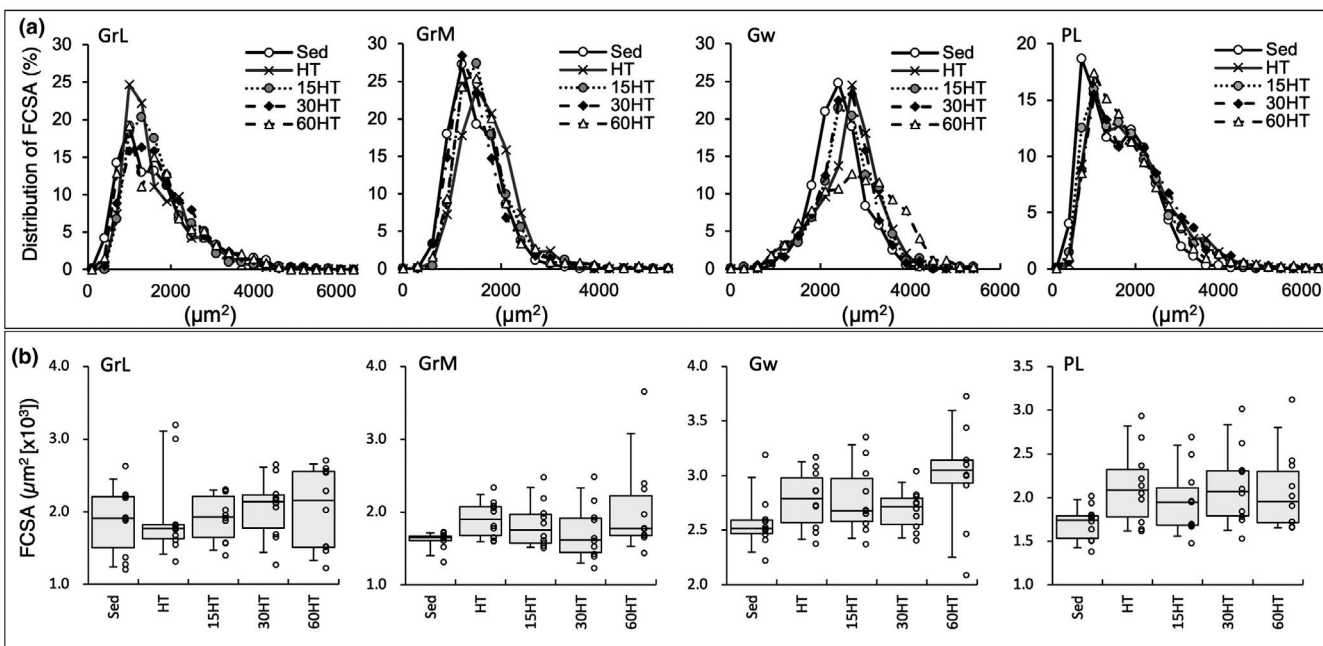
FIGURE 12 Distribution of FCSA (a) and total FCSA (b) values. Values are expressed as box and whisker plots with 5th, 25th, 50th, 75th and 95th percentile. Dots are individual data points in the panel (b).
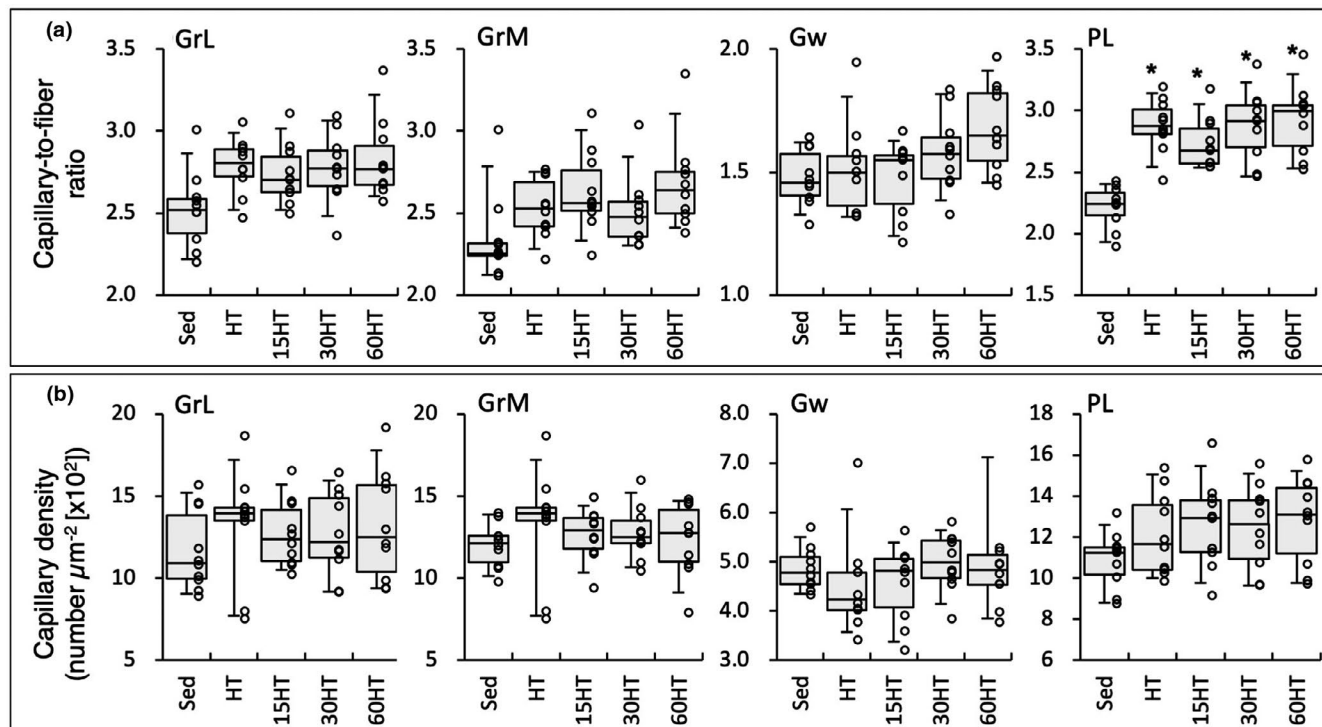
FIGURE 13 Capillary-to-fiber ratio (a) and capillary density (b) values. Values are expressed as box and whisker plots with 5th, 25th, 50th, 75th and 95th percentile. Dots are individual data points. *, significantly different from the Sed group.

(Goodwin & Taegtmeyer, 2000). Plasma fatty acid levels have been shown to increase during exercise (Friedberg et al. 1963). Thus, these findings may indicate that fatty acid oxidation in cardiac muscle is facilitated during intensive exercise, i.e., at high concentrations of blood lactate and free fatty acids. In the present study, LDH activity values in LV were markedly reduced in 30HT and 60HT groups (Figure 7b). This result may show that lactate oxidation in the heart was reduced and thereby the plasma lactate concentration may have been higher in these two groups than in the other groups during exercise. As mentioned above, in 60HT, but not 30HT, fatty acid metabolism was markedly improved in LV, thereby increasing the capacity of the heart to generate ATP via fatty acid oxidation during intensive exercise. Furthermore, CPT2 activity levels were remarkably upregulated by 60HT in Gr and PL (Figure 5B). Thus, HT with daily hyperbaric exposure for 60 min has the potential to further increase exercise performance by facilitating fatty acid metabolism in cardiac muscle.

Although significant changes were not observed, HT with hyperbaric exposure markedly upregulated DRP1 levels in LV (from 1.6- to 1.8-fold greater than HT group, Figure 8a). DRP1 inhibition was shown to suppress mitochondrial respiration and reactive oxygen species without morphological changes in mitochondria, i.e. fission, in rat cardiomyocytes (Zhang et al. 2017). After acute exercise, mitochondrial fission was markedly observed in cardiac muscle (Coronado et al. 2018). In vascular smooth muscle

cells, mitochondrial fission induced by platelet-derived growth factor was shown to enhance fatty acid oxidation and suppress glucose oxidation (Salabei & Hill, 2013). In the present study, levels of DRP1 were significantly correlated with COX, CS and HAD activity values in LV (Table 2). Thus, a modest increase in DRP1 levels may induce mitochondrial fission and contribute to promoting fatty acid metabolism in cardiac muscle.

While hyperbaric exposure did not cause an additive effect, AKT1 levels were significantly increased in the four training groups in PL (Figure 9b). A positive correlation was observed between AKT1 levels and FCSA values in PL (Table 2). Thus, hybrid training used in the present study caused muscle fiber hypertrophy, possibly via AKT1 upregulation. AKT1 was shown to promote muscle growth via facilitating satellite cell proliferation during skeletal muscle hypertrophy (Moriya et al. 2018). In Gw, a significant correlation was observed between total FCSA and HSP70 levels, but not with AKT1 levels (Table 2). Mean values of HSP70 levels in Gw were markedly greater in 30HT (1.4-fold) and 60HT (1.6-fold) groups than in the HT group. This is consistent with previous findings using untrained (Suzuki, 2017) and highly trained mice (Suzuki, 2019A). HSP70 was shown to play an important role in the recovery of striated muscle after severe exercise (McArdle et al. 2004). Recovery from muscle damage induced by daily exercise may be facilitated by hyperbaric exposure-induced HSP70 upregulation, resulting in the promotion of muscular adaptation to exercise training.

Muscle capillary geometry was markedly improved by HT irrespective of hyperbaric exposure in PL (Figure 13). A positive correlation was noted between C:F ratios and AKT1 levels in PL (Table 2). In muscle-specific inducible AKT1 transgenic mice, the C:F ratio was significantly increased in soleus muscle (Onoue et al. 2018). Thus, promoted levels of AKT1 by HT may contribute to improve muscle capillary network in highly trained mice.

ACKNOWLEDGMENTS

CONFLICT OF INTEREST

None declared.

AUTHOR CONTRIBUTION

The author J.S. was involved in the conception and design of the study, analyzing the data, and preparing the first draft of the manuscript. The author revised the draft manuscript and approved the final concept. The author agrees to be accountable for all aspects of the work in ensuring questions relating to the accuracy and integrity of any part of the work are appropriately investigated and resolved.

ORCID

Junichi Suzuki https://orcid.org/0000-0003-0271-2071

REFERENCES

Allard, M. F., Schonekess, B. O., Henning, S. L., English, D. R., & Lopaschuk, G. D. (1994). Contribution of oxidative metabolism and glycolysis to ATP production in hypertrophied hearts. *American Journal of Physiology-Heart and Circulatory Physiology*, *267*, H742–H750.

Ballmann, C., Tang, Y., Bush, Z., & Rowe, G. C. (2016). Adult expression of PGC-1α and -1β in skeletal muscle is not required for endurance exercise-induced enhancement of exercise capacity. *American Journal of Physiology-Endocrinology and Metabolism*, *311*, E928–E938.

Bass, A., Brdiczka, D., Eyer, P., Hofer, S., & Pette, D. (1969). Metabolic differentiation of distinct muscle types at the level of enzymatic organization. *European Journal of Biochemistry*, *10*, 198–206.

Brandt, N., Dethlefsen, M. M., Bangsbo, J., & Pilegaard, H. (2017). PGC-1α and exercise intensity dependent adaptations in mouse skeletal muscle. *PLoS One*, *12*, 1–21.

Carnevali, J. C., Eder, R., Lira, F. S., Lima, W. P., Gonçalves, D. C., Zanchi, N. E., Nicastro, H., Laboie, J. M., & Seelander, M. C. L. (2012). Effects of high-intensity intermittent training on carnitine palmitoyl transferase activity in the gastrocnemius muscle of rats. *Brazilian Journal of Medical and Biological Research*, *45*, 777–783.

Coronado, M., Fajardo, G., Nguyen, K., Zhao, M., Kooiker, K., & Jung, G. (2018). Physiological mitochondrial fragmentation is a normal cardiac adaptation to increased energy demand. *Circulation Research*, *122*, 282–295.

Czubryt, M. P., McAnally, J., Fishman, G. I., & Olson, E. N. (2003). Regulation of peroxisome proliferator-activated receptor gamma coactivator 1 alpha (PGC-1 alpha) and mitochondrial function by MEF2 and HDAC5. *Proceedings of the National Academy of Sciences of the United States of America*, *100*, 1711–1716.

Friedberg, S. J., Sher, P. B., Bogdonoff, M. D., & Estes, E. H. (1963). The dynamics of plasma free fatty acid metabolism during exercise. *Journal of Lipid Research*, *4*, 34–38.

Gibb, A. A., & Hill, B. G. (2018). Metabolic coordination of physiological and pathological cardiac remodeling. *Circulation Research*, *123*, 107–128.

Gilda, J. E., & Gomes, A. V. (2013). Stain-Free total protein staining is a superior loading control to β-actin for Western blots. *Analytical Biochemistry*, *440*, 186–188.

Goodwin, G. W., & Taegtmeyer, H. (2000). Improved energy homeostasis of the heart in the metabolic state of exercise. *American Journal of Physiology - Heart and Circulatory Physiology*, *279*, H1490–H1501.

Hafstad, A. D., Boardman, N. T., Lund, J., Hagve, M., Khalid, A. M., & Wisløff, U. (2011). High intensity interval training alters substrate utilization and reduces oxygen consumption in the heart. *Journal of Applied Physiology*, *111*, 1235–1241.

Ke, C. J., He, Y. H., He, H. W., Yang, X., Li, R., & Yuan, J. (2014). A new spectrophotometric assay for measuring pyruvate dehydrogenase complex activity: A comparative evaluation. *Analytical Methods*, *6*, 6381–6638.

Kemppainen, J., Fujimoto, T., Kalliokoski, K. K., Viljanen, T., Nuutila, P., & Knuuti, J. (2002). Myocardial and skeletal muscle glucose uptake during exercise in humans. *Journal of Physiology*, *542*, 403–412.

Kruschke J. K. (2015). *Bayesian data analysis. A tutorial with R, JAGS and Stan*, (2nd ed.). Elsevier Inc.

Kruschke, J. K. (2018). Rejecting or accepting parameter values in Bayesian estimation. *Advances in Methods and Practices in Psychological Science*, *1*, 270–280.

Kruschke, J. K., & Liddell, T. M. (2018). Bayesian data analysis for newcomers. *Psychonomic Bulletin & Review*, *25*, 155–177.

McArdle, A., Dillmann, W. H., Mestril, R., Faulkner, J. A., & Jackson, M. J. (2004). Overexpression of HSP70 in mouse skeletal muscle protects against muscle damage and age-related muscle dysfunction. *The FASEB Journal*, *18*, 355–357.

Moriya, N., & Miyazaki, M. (2018). Akt1 deficiency diminishes skeletal muscle hypertrophy by reducing satellite cell proliferation. *American Journal of Physiology - Regulatory, Integrative and Comparative Physiology*, *314*, R741–R751.

Onoue, Y., Izumiya, Y., Hanatani, S., Ishida, T., Arima, Y., & Yamamura, S. (2018). Akt1-mediated muscle growth promotes blood flow recovery after hindlimb ischemia by enhancing heme oxygenase-1 in neighboring cells. *Circulation Journal*, *82*, 2905–2912.

Park, S., Park, S., Shin, M., & Kim, C. (2018). The effects of low-pressure hyperbaric oxygen treatment before and after maximal exercise on lactate concentration, heart rate recovery, and antioxidant capacity. *Journal of Exercise Rehabilitation*, *14*, 980–984.

Passonneau, J. V., & Lowry, O. H. *Enzymatic analysis: A practical guide*, Humana press. 1993.

Risso, G., Blaustein, M., Pozzi, B., Mammi, P., & Srebrow, A. (2015). Akt/PKB: One kinase, many modifications. *The Biochemical Journal*, *468*, 203–214.

Salabei, J. K., & Hill, B. G. (2013). Mitochondrial fission induced by platelet-derived growth factor regulates vascular smooth muscle cell bioenergetics and cell proliferation. *Redox Biology*, *1*, 542–551.

Schönekess, B. O. (1997). Competition between lactate and fatty acids as sources of ATP in the isolated working rat heart. *Journal of Molecular and Cellular Cardiology*, 29, 2725–2733.

Sherratt, H. S. A., Watmough, N. J., Johnson, M. A., & Turnbull, D. M. (1988). Methods for study of normal and abnormal skeletal muscle mitochondria. In D. Glick (Ed.), *Methods of biochemical analysis* (Vol. 33, pp. 270–271). Interscience Publishers Inc.

Skovgaard, C., Brandt, N., Pilegaard, H., & Bangsbo, J. (2016). Combined speed endurance and endurance exercise amplify the exercise-induced PGC-1a and PDK4 mRNA response in trained human muscle. *Physiological Reports*, 4, e12864.

Srere, P. A. (1969). Citrate synthase. *Methods in Enzymology*, 1, 3–5.

Suzuki, J. (2017). Endurance performance is enhanced by intermittent hyperbaric exposure via up-regulation of proteins involved in mitochondrial biogenesis in mice. *Physiological Reports*, 5, e13349.

Suzuki, J. (2019a). Effects of intermittent hyperbaric exposure on endurance and interval exercise performance in well-trained mice. *Experimental Physiology*, 104, EP087360.

Suzuki, J. (2019b). Effects of exercise training with short-duration intermittent hypoxia on endurance performance and muscle metabolism in well-trained mice. *Physiological Reports*, 7, e14182.

Terblanche, S. E., Gohil, K., Packer, L., Henderson, S., & Brooks, G. A. (2001). The effects of endurance training and exhaustive exercise on mitochondrial enzymes in tissues of the rat (Rattus norvegicus). *Comparative Biochemistry and Physiology - Part A: Molecular & Integrative Physiology*, 128, 889–896.

Vega, R. B., Huss, J. M., & Kelly, D. P. (2000). The coactivator PGC-1 cooperates with peroxisome proliferator-activated receptor alpha in transcriptional control of nuclear genes encoding mitochondrial fatty acid oxidation enzymes. *Molecular and Cellular Biology*, 20, 1868–1876.

Vigelsø, A., Dybboe, R., Hansen, C. N., Dela, F., Helge, J. W., & Guadalupe-Grau, A. (2014). GAPDH and β-actin protein decreases with aging making Stain-Free technology a superior loading control in Western Blotting of human skeletal muscle. *Journal of Applied Physiology*, 118, 386–394.

Wasserstein, R. L., & Lazar, N. A. (2016). The ASA's statement on *p*-Values: Context, process, and purpose. *American Statistician*, 70, 129–133.

Wen, X., Wu, J., Chang, J. S., Zhang, P., Wang, J., Zhang, Y., Gettys, T. W., & Zhang, Y. Effect of exercise intensity on isoform-specific expressions of NT-PGC-1 α mRNA in mouse skeletal muscle. *BioMed Research International*, 2014, 402175.

Yuan, H., Niu, Y., Liu, X., & Fu, L. (2014). Exercise increases the binding of MEF2A to the Cpt1b promoter in mouse skeletal muscle. *Acta Physiologica*, 212, 283–292.

Zhang, L., Zhou, Y., Wu, W., Hou, L., Chen, H., & Zuo, B. (2017). Skeletal muscle-specific overexpression of PGC-1α induces fiber-type conversion through enhanced mitochondrial respiration and fatty acid oxidation in mice and pigs. *International Journal of Biological Sciences*, 13, 1152–1162.

SUPPORTING INFORMATION

Additional supporting information may be found online in the Supporting Information section.

How to cite this article: Suzuki J. Effects of hyperbaric environment on endurance and metabolism are exposure time-dependent in well-trained mice. *Physiol Rep*. 2021;9:e14780. https://doi.org/10.14814/phy2.14780